Supporting Information

Carbamoyl Azide-Drug Conjugates as Supramolecular Gelators: Design, Synthesis, Crystal Structures and Anti-Melanoma Property

Manoj Kumar Baskey[a], Subhajit Ghosh[a], Sabir Ahmed[a] and Parthasarathi Dastidar[a]*

[a]School of Chemical Sciences, Indian Association for the Cultivation of Science (IACS), 2A and 2B, Raja S. C. Mullick Road, Jadavpur, Kolkata - 700032, West Bengal, India

*e-mail: ocpd@iacs.res.in

Table of Contents

Sl. No.	Contents	Page no.
1.	Carbamoyl azide synthesis (scheme **1**)	2
2.	^{1}H NMR and ^{13}C NMR of carbamoyl azides(Fig. **S1-S10**)	2-7
3.	HR-Mass of Carbamoyl azides(Fig. **S11-S15**)	7-9
4.	FT-IR of all azide and corresponding precursor acids(Fig. **S16**)	10
5.	Single Crystal XRD analysis(Tab. **S1,** Fig. **S17**- Tab. **S6,** Fig. **S21**)	10-14
6.	Reaction scheme and mechanism(Fig. **S22**)	15
7.	PXRD plots of azides(bulk vs. simulated) (Fig. **S23**)	16
8.	Gelation, M.G.C and tanδ (G"/G') table (Tab. **S7**- Tab. **S8**)	16-17
9.	Rheological Experiments of gels(Fig. **S24**)	17
10.	FT-IR spectra of xerogel and Xerogel-incubated of Diclo-Az(Fig. **S25**)	18
11.	PXRD Patterns (xerogel vs. bulk, xerogel vs. simulated) (Fig. **S26**)	19
12.	Biological Studies(Fig. **S27**)	20
13.	Rheo-reversibility of Nap-Az (4 wt %, DMSO/water, 1:1:, v/v) (Fig. **S28**)	20

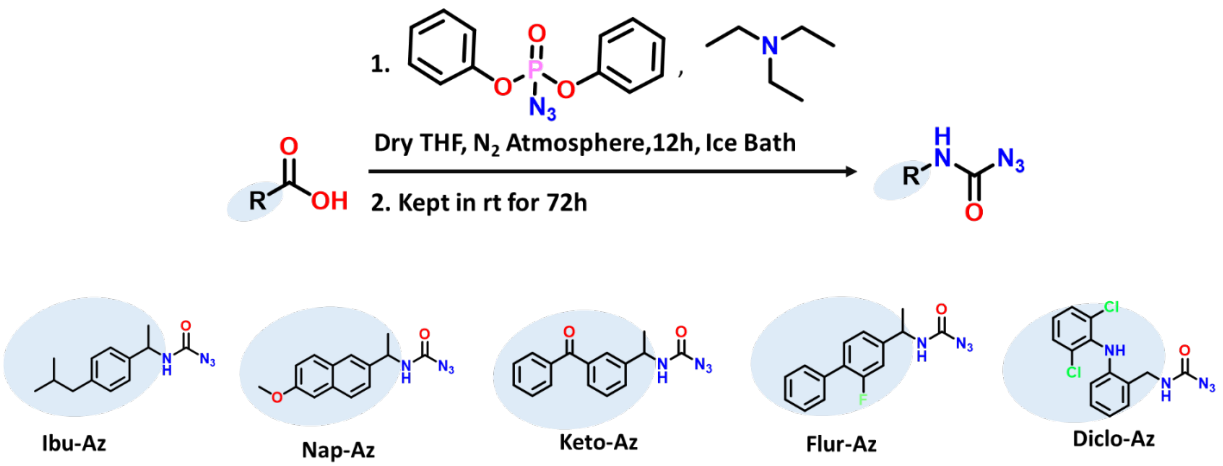

Scheme 1: Synthetic strategy for carbamoyl azide **Ibu-Az, Nap-Az, Keto-Az, Flur-Az** and **Diclo-Az.**

Caution: Carbamoyl azides are sensitive to excessive heat and shock as they have potential for explosive decomposition and therefore, these compounds should be handled with care.

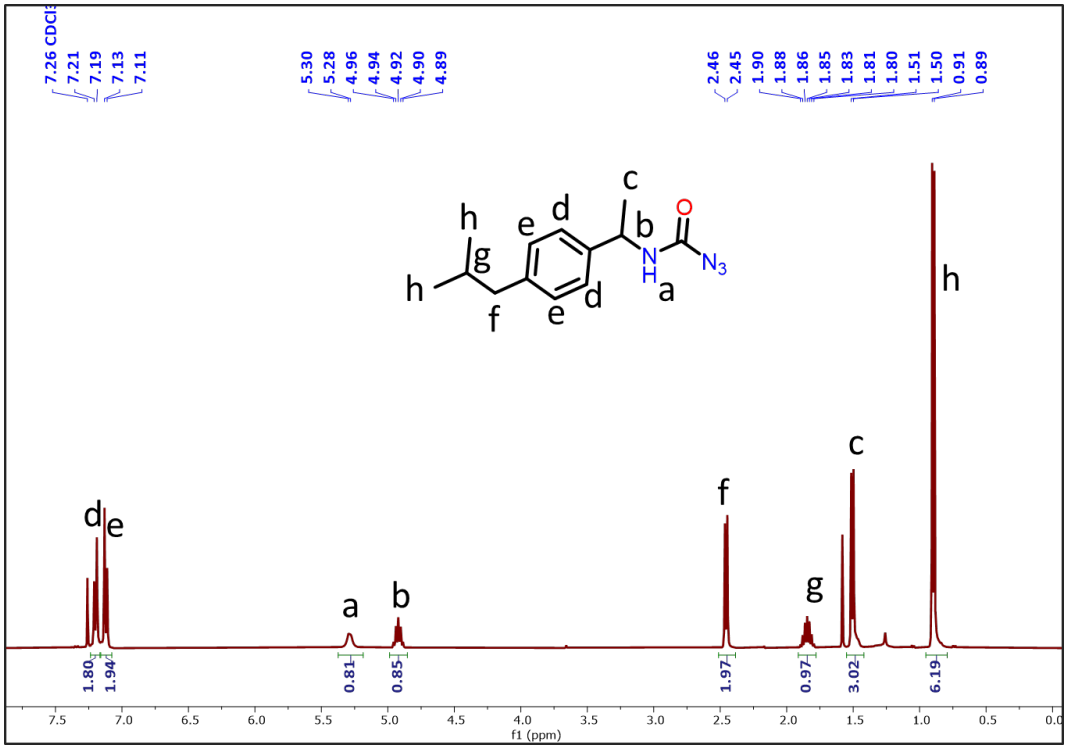

Fig. S1 : ^{1}H NMR of **Ibu-Az** in $CDCl_3$.

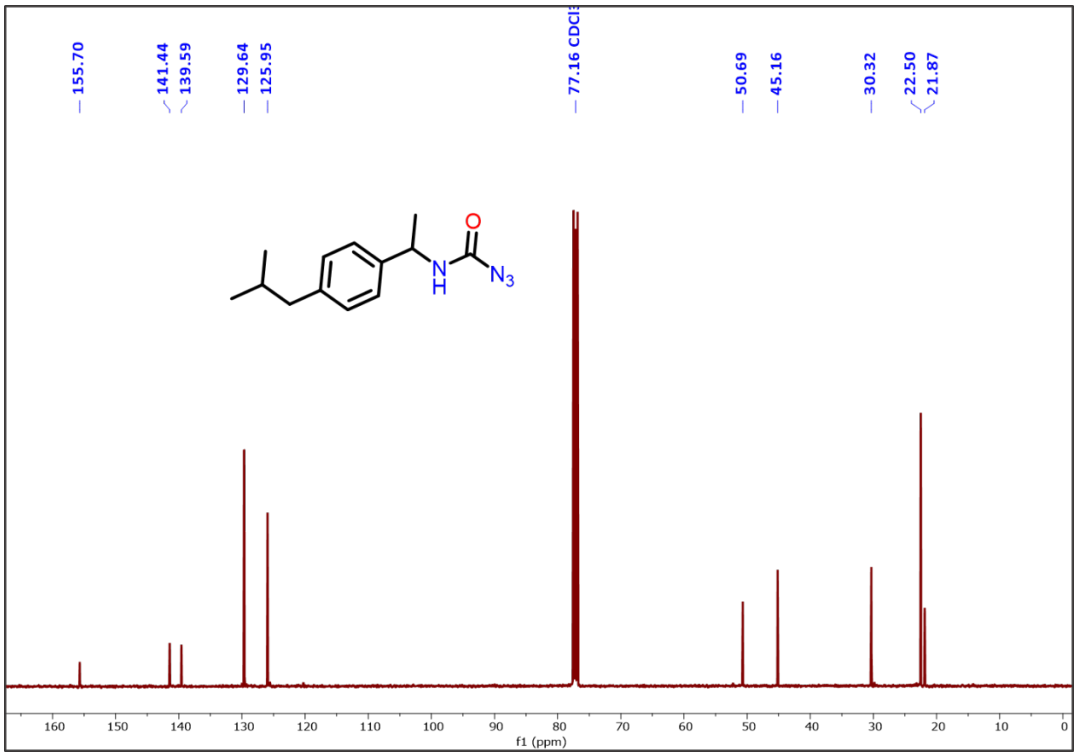

Fig. S2: ^{13}C NMR of **Ibu-Az** in $CDCl_3$.

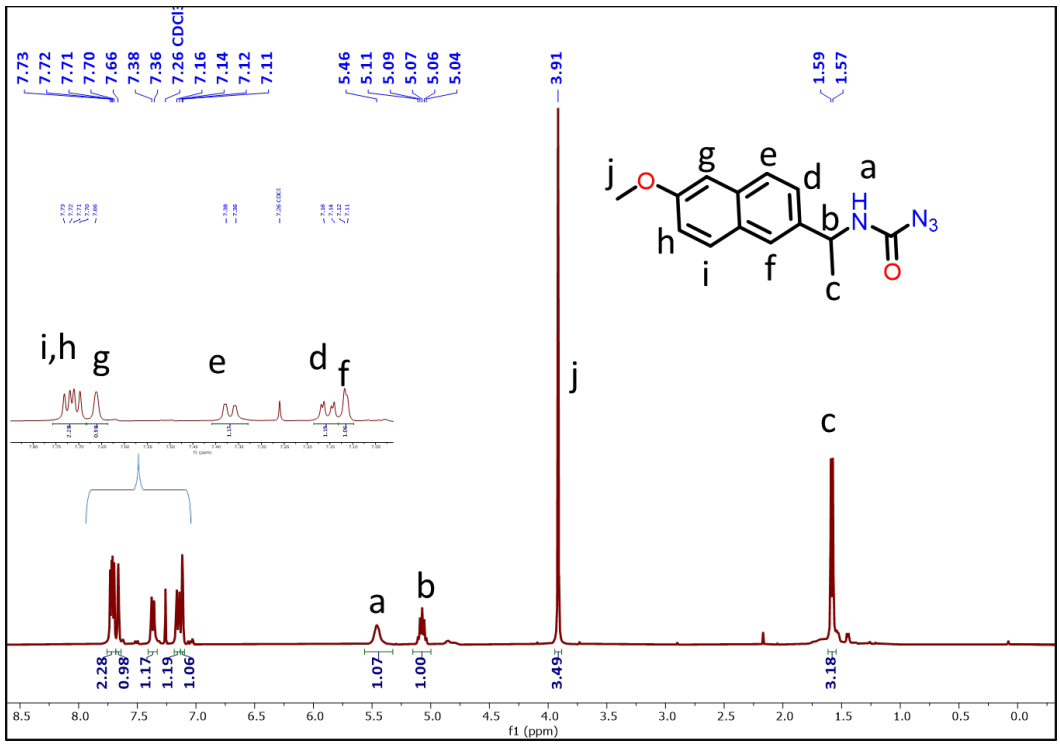

Fig. S3: ^{1}H NMR of **Nap-Az** in $CDCl_3$.

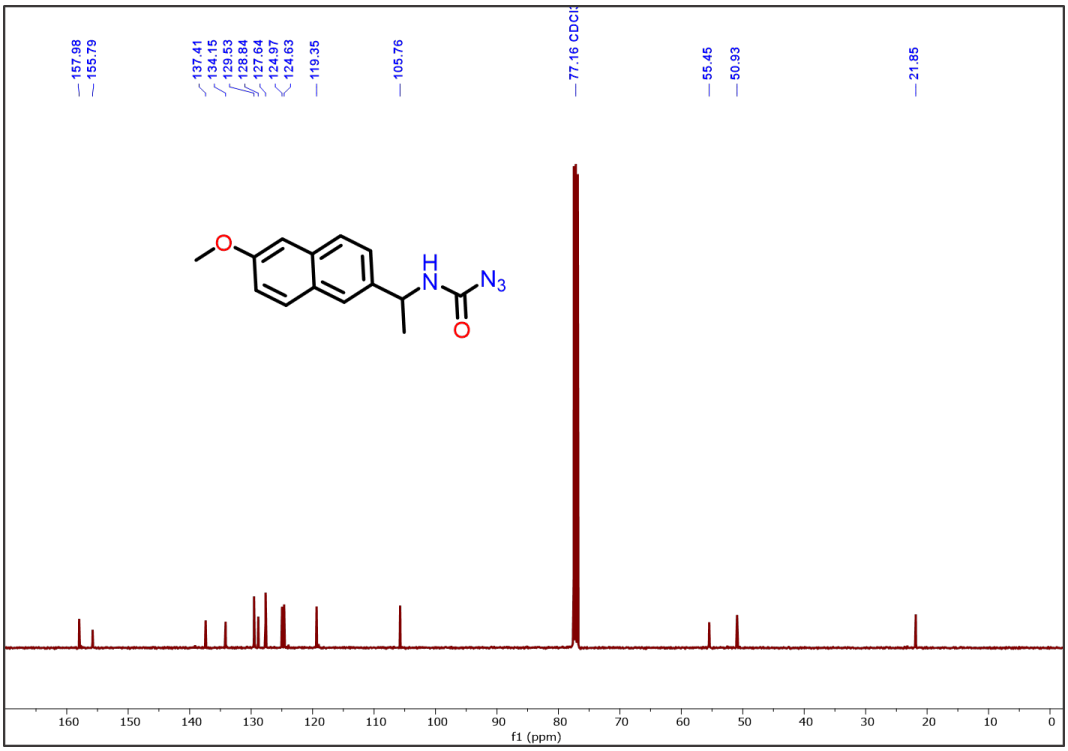

Fig. S4: ^{13}C NMR of **Nap-Az** in $CDCl_3$.

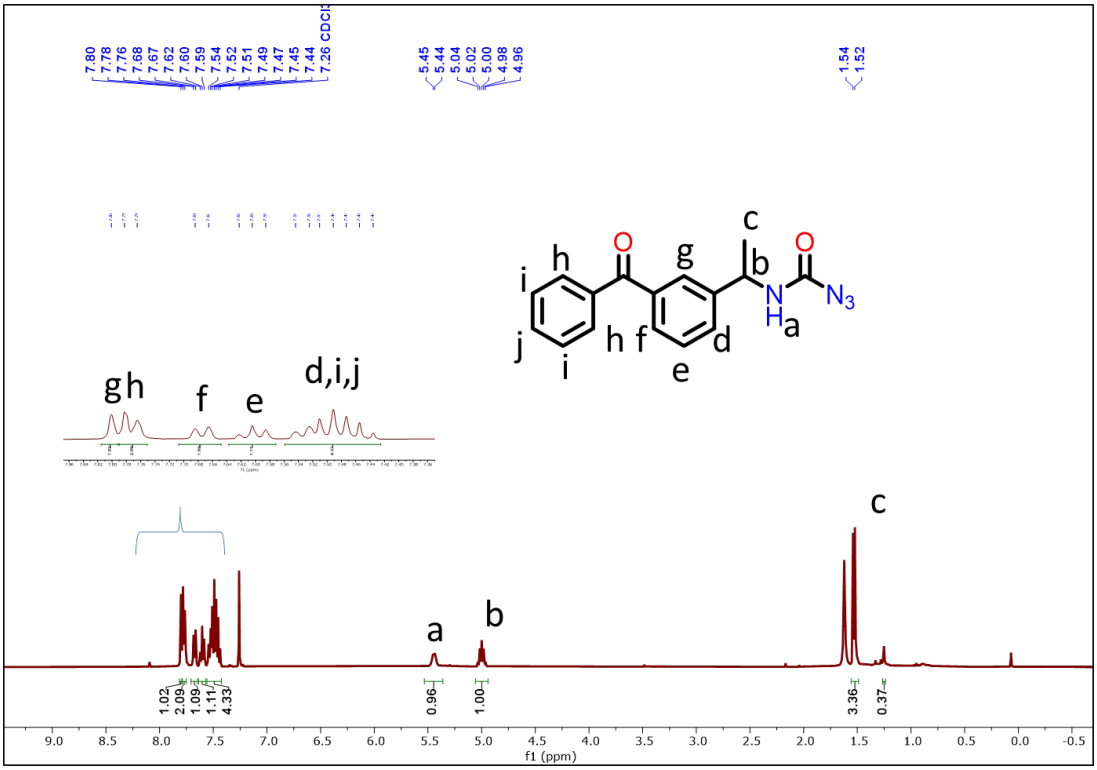

Fig. S5: ^{1}H NMR of **Keto-Az** in $CDCl_3$.

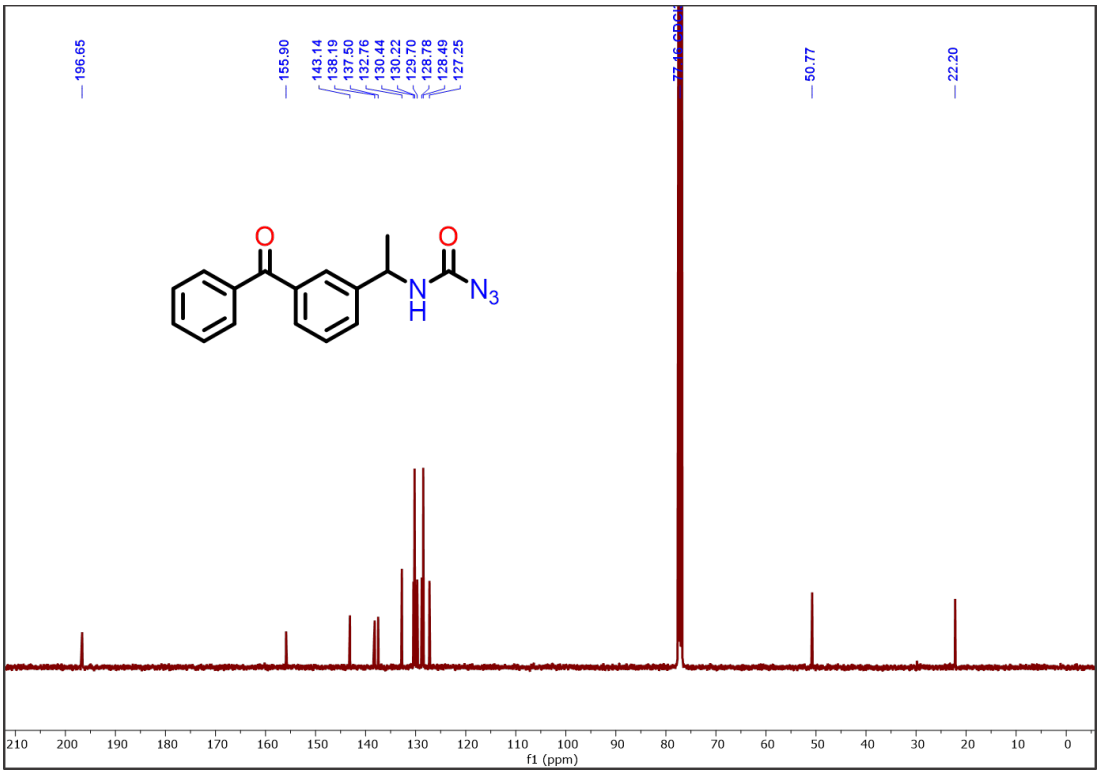

Fig. S6: ^{13}C NMR of **Keto-Az** in $CDCl_3$.

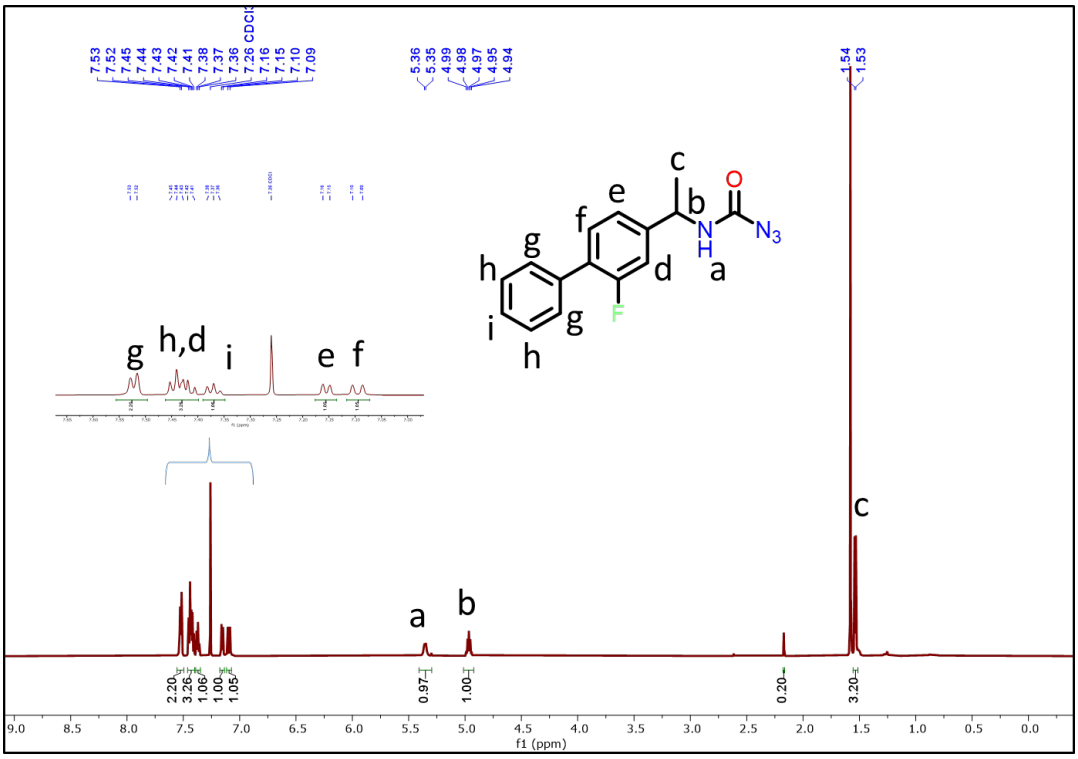

Fig. S7: ^{1}H NMR of **Flur-Az** in $CDCl_3$.

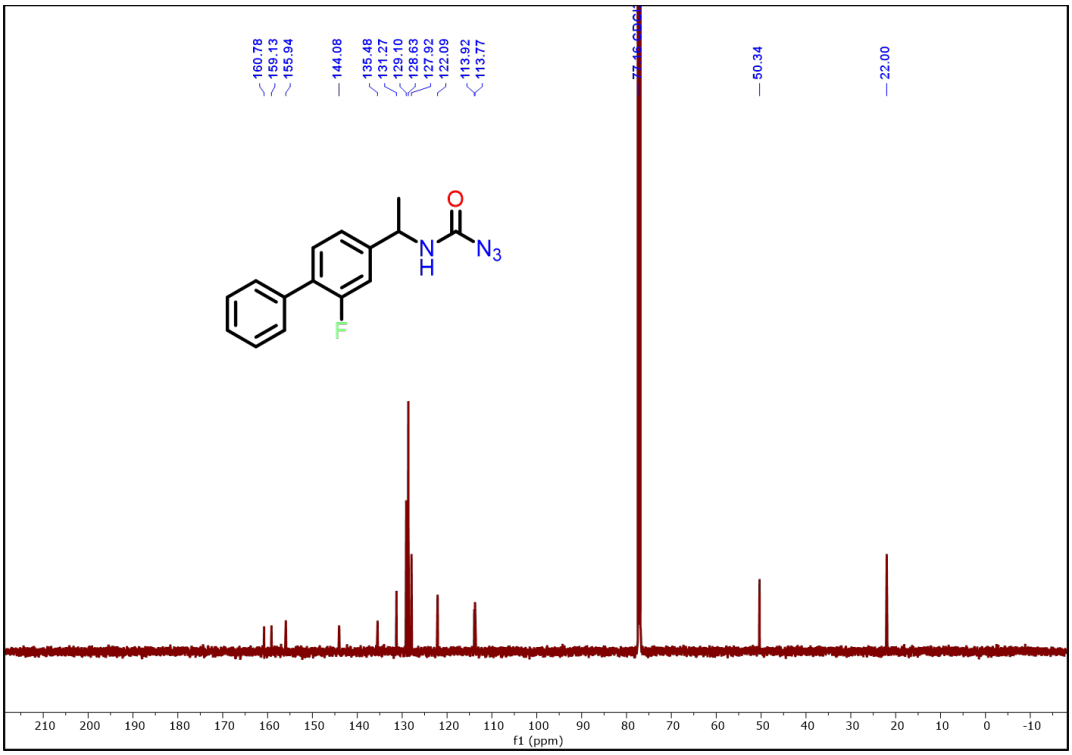

Fig. S8: ^{13}C NMR of **Flur-Az** in $CDCl_3$.

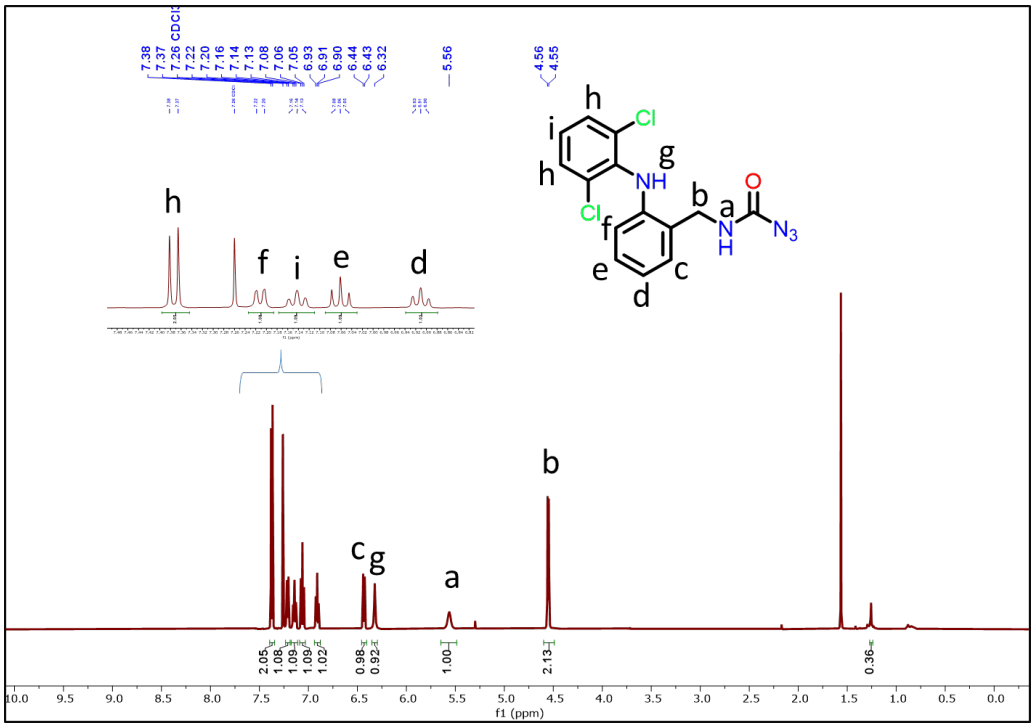

Fig. S9: ^{1}H NMR of **Diclo-Az** in $CDCl_3$.

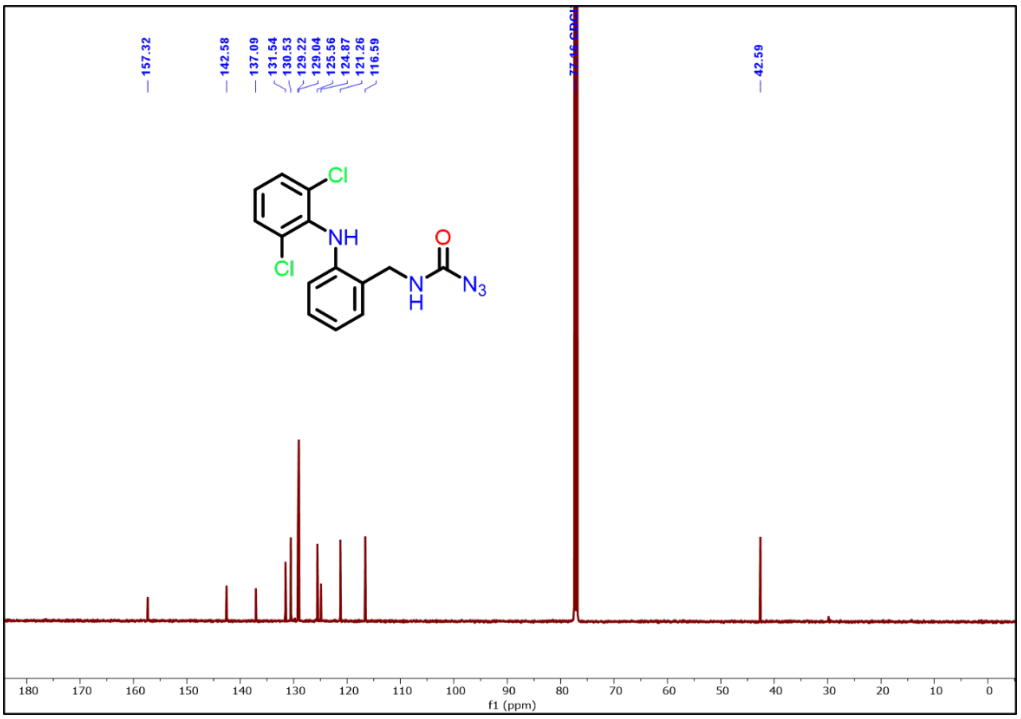

Fig. S10: ^{13}C NMR of **Diclo-Az** in $CDCl_3$.

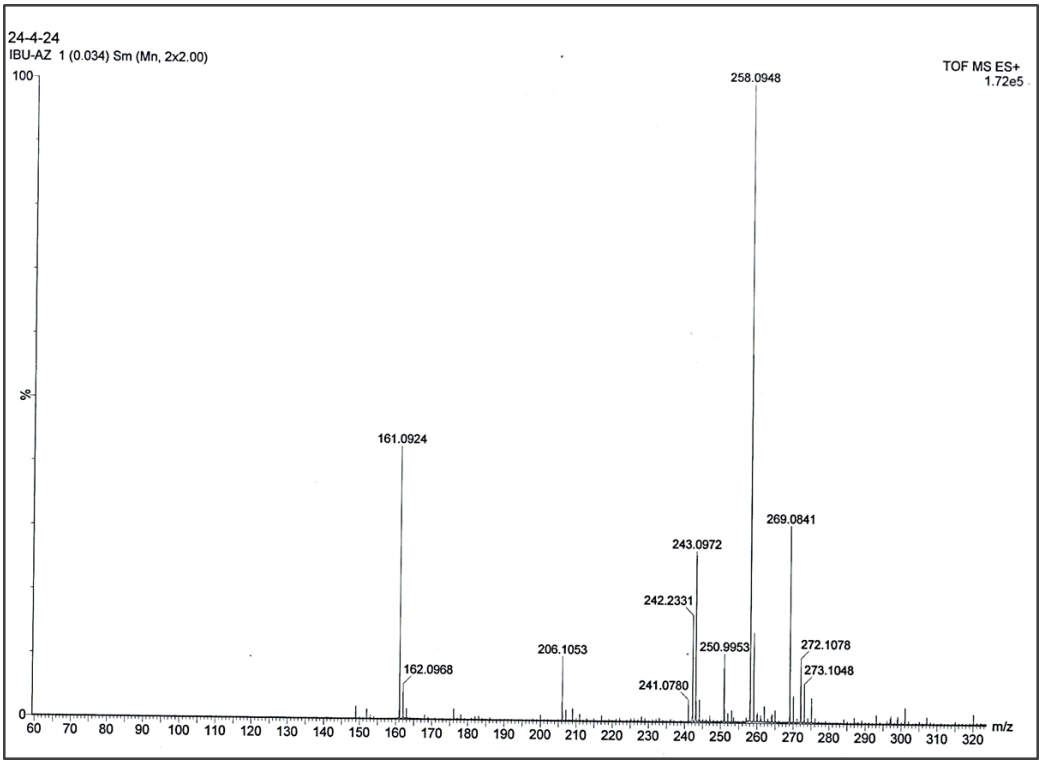

Fig. S11: HR-MASS of **Ibu-Az** obtained at $[M+Na]^+$=269.08 m/z

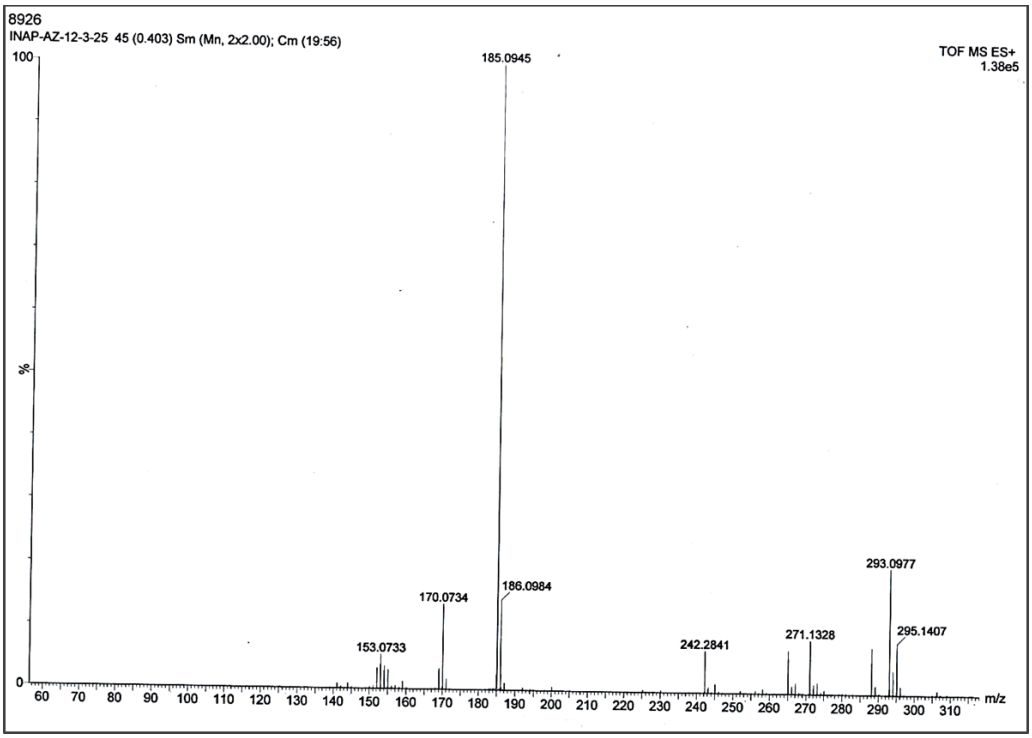

Fig. S12: HR-MASS of **Nap-Az** obtained at $[M+Na]^+$=293.09 m/z

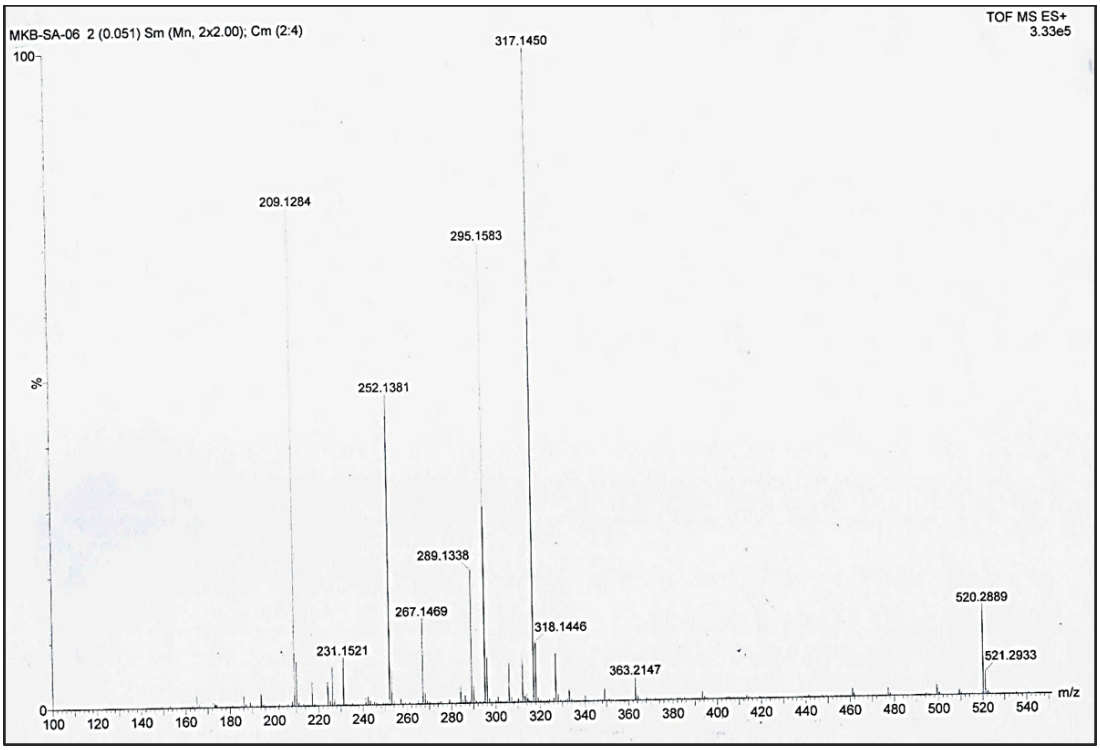

Fig. S13: HR-MASS of **Keto-Az** obtained at $[M+Na]^+$=317.14 m/z

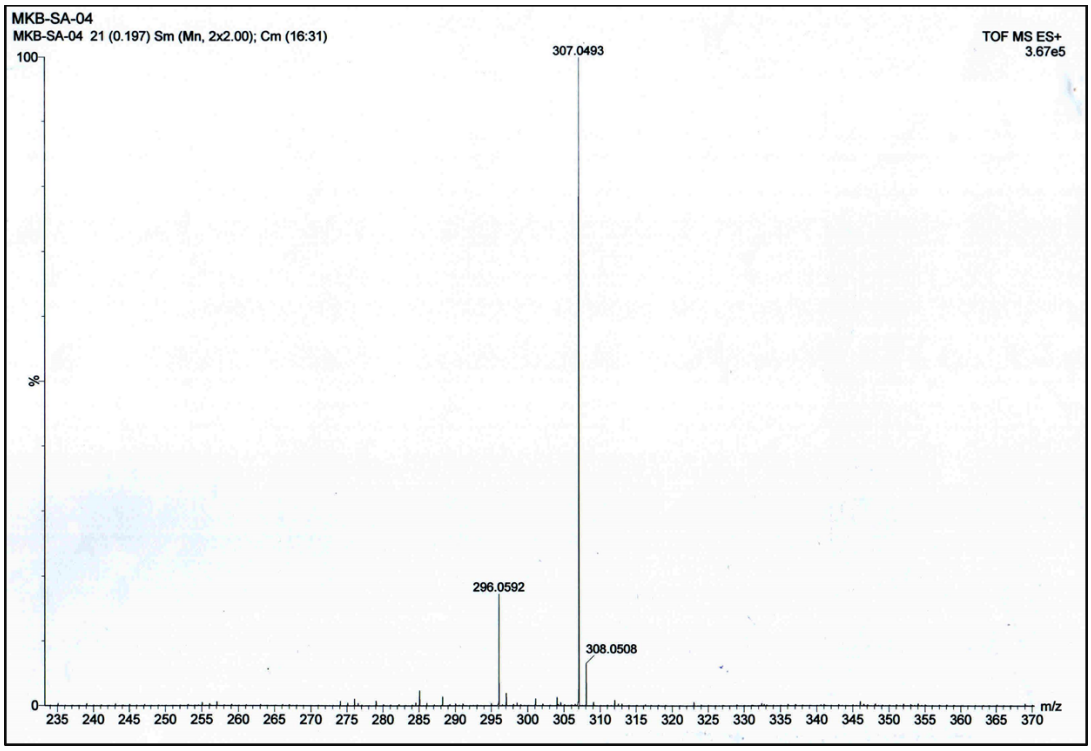

Fig. S14: HR-MASS of **Flur-Az** obtained at $[M+Na]^+$=307.04 m/z

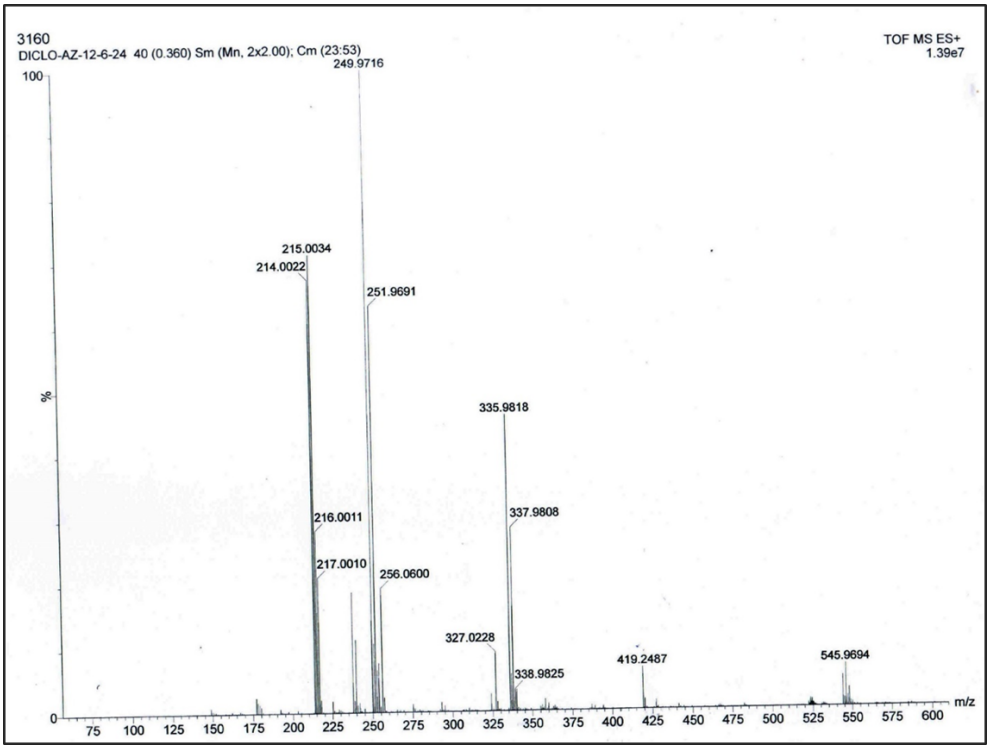

Fig. S15: HR-MASS of **Diclo-Az** obtained at $[M+H]^+$=335.98 m/z

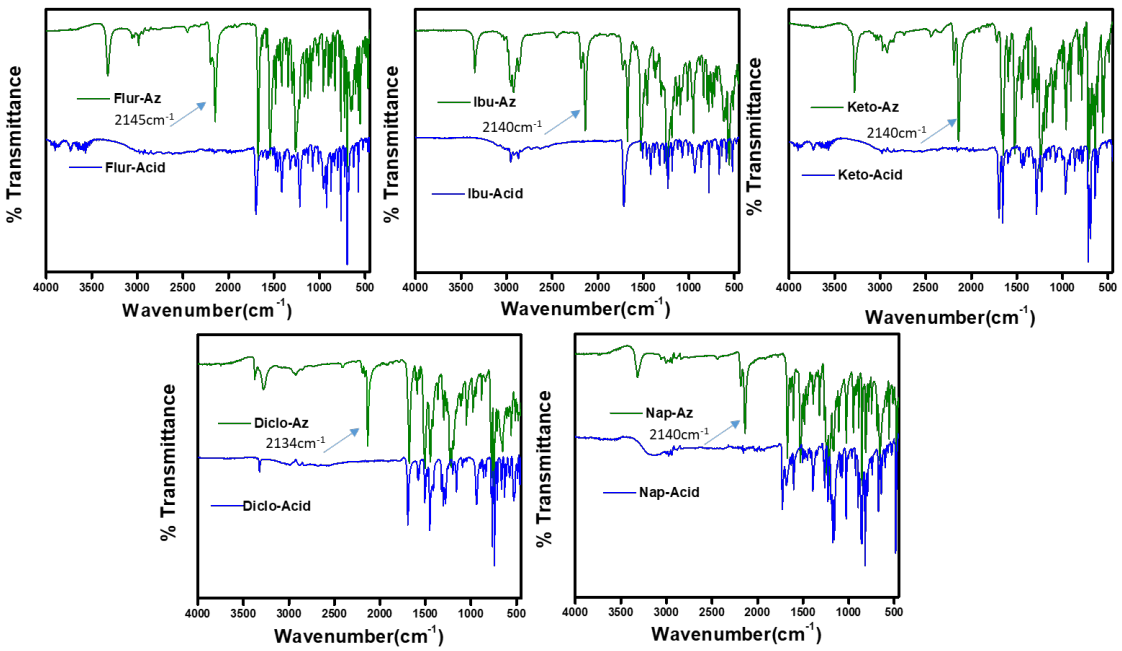

Fig. S16: FT-IR spectra of azides and corresponding precursor acids.

Table S1: Crystallographic data table:

Identification Code	**Ibu-Az**	**Nap-Az**	**Keto-Az**	**Flur-Az**	**Diclo-Az**
CCDC number	2049306	2049307	2432622	2049308	2362781
Empirical formula	$C_{13}H_{18}N_4O$	$C_{14}H_{14}N_4O_2$	$C_{16}H_{14}N_4O_2$	$C_{30}H_{23}F_2N_8O_2$	$C_{14}H_{11}Cl_2N_5O$
Formula weight	246.31	270.29	294.31	565.56	336.18
Temperature/K	110.46	120.1	159.97	124.38	150.0
Crystal system	triclinic	monoclinic	monoclinic	triclinic	monoclinic
Space group	*P*-1	$P2_1/c$	$P2_1/c$	*P*-1	$P2_1/c$
a/Å	5.207(2)	13.9443(10)	19.98(2)	6.516(2)	14.073(9)
b/Å	11.084(6)	5.2071(4)	4.808(5)	10.111(3)	4.879(3)
c/Å	11.850(5)	18.4952(12)	14.863(12)	21.318(7)	22.444(14)

α/°	98.187(17)	90	90	91.568(5)	90
β/°	97.794(15)	94.240(2)	91.84(4)	92.708(5)	98.92(2)
γ/°	95.548(17)	90	90	103.339(5)	90
Volume/Å^3	665.9(6)	1339.25(17)	1427(2)	1363.9(8)	1522.2(16)
Z	2	4	4	2	4
ρ_{calc}g/cm^3	1.228	1.341	1.370	1.377	1.467
μ/mm^{-1}	0.082	0.094	0.094	0.100	0.435
F(000)	264.0	568.0	616.0	586.0	688.0
Crystal size/mm^3	0.18 × 0.16 × 0.12	0.2 × 0.18 × 0.14	0.06 × 0.04 × 0.04	0.2 × 0.18 × 0.12	0.12 × 0.07 × 0.05
Radiation	MoKα (λ = 0.71073)	MoKα (λ = 0.71073)	MoKα (λ = 0.71073)	MoKα (λ = 0.71073)	MoKα (λ = 0.71073)
2Θ range for data collection/°	4.71 to 47.322	5.116 to 54.196	5.484 to 50.092	1.914 to 45.972	5.86 to 50.182
Index ranges	-5 ≤ h ≤ 5, -12 ≤ k ≤ 12, -13 ≤ l ≤ 13	-17 ≤ h ≤ 17, -6 ≤ k ≤ 6, -23 ≤ l ≤ 23	-23 ≤ h ≤ 23, 0 ≤ k ≤ 5, 0 ≤ l ≤ 17	-7 ≤ h ≤ 7, -11 ≤ k ≤ 11, -23 ≤ l ≤ 23	-16 ≤ h ≤ 16, -5 ≤ k ≤ 5, -26 ≤ l ≤ 26
Reflections collected	5569	13240	2507	20695	12467
Independent reflections	1995 [R_{int} = 0.0910, R_{sigma} = 0.1027]	2946 [R_{int} = 0.0822, R_{sigma} = 0.0700]	2507 [R_{int} = 0.075, R_{sigma} = 0.1779]	3779 [R_{int} = 0.1276, R_{sigma} = 0.0985]	2695 [R_{int} = 0.0957, R_{sigma} = 0.0773]
Data/restraints/parameters	1995/0/166	2946/0/183	2507/0/201	3779/0/385	2695/0/199
Goodness-of-fit on F^2	1.036	1.051	1.026	1.141	1.031
Final R indexes [I>=2σ (I)]	R_1 = 0.0647, wR_2 = 0.1646	R_1 = 0.0487, wR_2 = 0.1227	R_1 = 0.1227, wR_2 = 0.3035	R_1 = 0.1198, wR_2 = 0.3398	R_1 = 0.0624, wR_2 = 0.1568
Final R indexes [all data]	R_1 = 0.0899, wR_2 = 0.1825	R_1 = 0.0649, wR_2 = 0.1323	R_1 = 0.1880, wR_2 = 0.3466	R_1 = 0.1869, wR_2 = 0.3780	R_1 = 0.0822, wR_2 = 0.1731
Largest diff. peak/hole / e Å^{-3}	0.23/-0.28	0.19/-0.24	0.42/-0.49	0.62/-0.45	0.40/-0.40

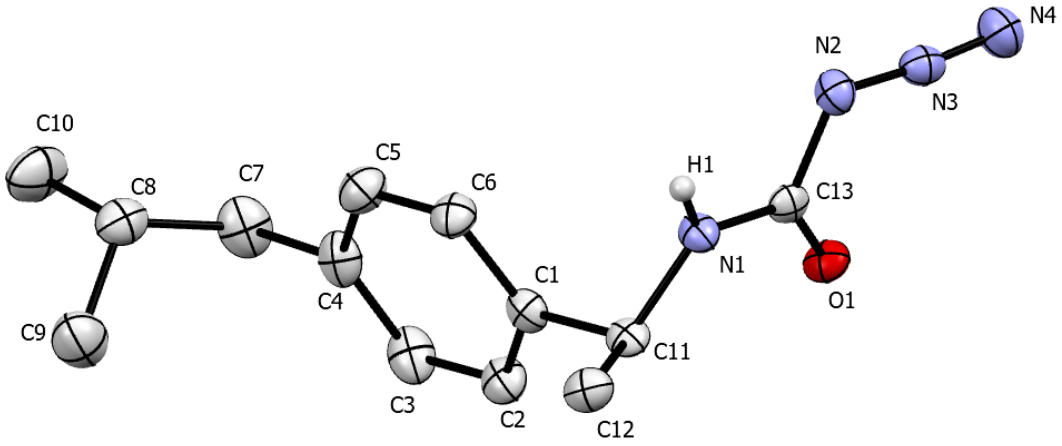

Fig. S17: ORTEP plot of **Ibu-Az** (50% probability)

Table S2: Hydrogen bonding table for **Ibu-Az**

D-H···A	d(D-H)/Å	d(H···A)/Å	d(D···A)/Å	∠D-H···A/°	Symmetry
N1--H1···O1	0.88	2.18	3.014(3)	157	-1+x,y,z

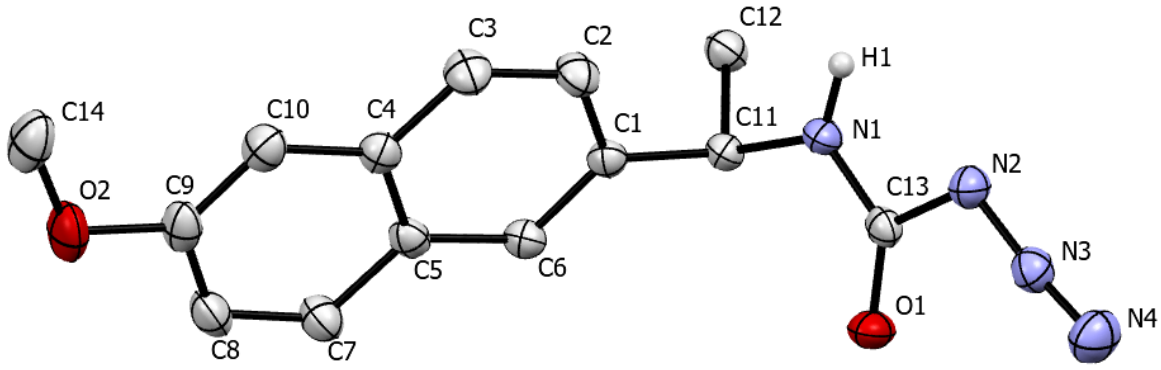

Fig. S18: ORTEP plot of **Nap-Az** (50% probability)

Table S3: Hydrogen bonding table for **Nap-Az**

D-H···A	d(D-H)/Å	d(H···A)/Å	d(D···A)/Å	∠D-H···A/°	Symmetry
N1-H1···O1	0.88	2.18	3.0253(19)	160	x,1+y,z

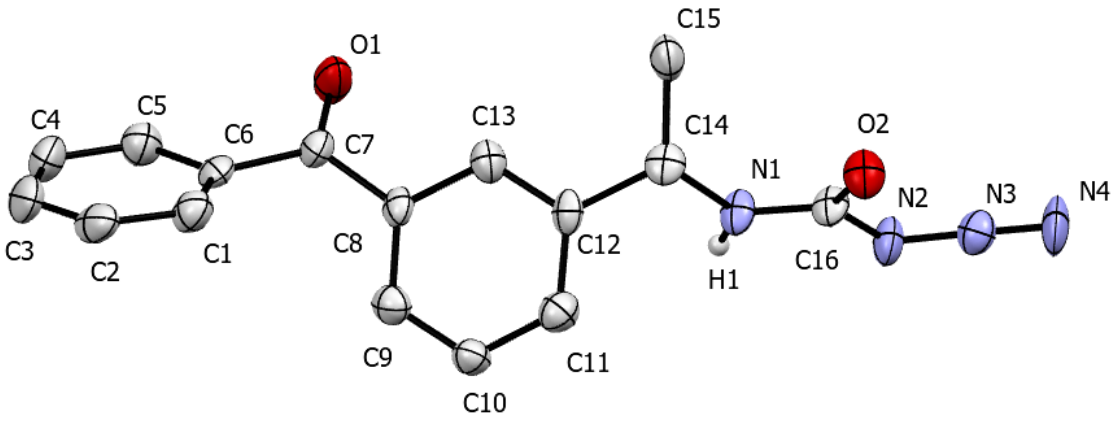

Fig. S19: ORTEP plot of **Keto-Az** (50% probability)

Table S4: Hydrogen bonding table for **Keto-Az**

D-H···A	d(D-H)/Å	d(H···A)/Å	d(D···A)/Å	∠D-H···A/°	Symmetry
N1-H1···O2	0.88	2.02	2.877(8)	165	x,-1+y,z

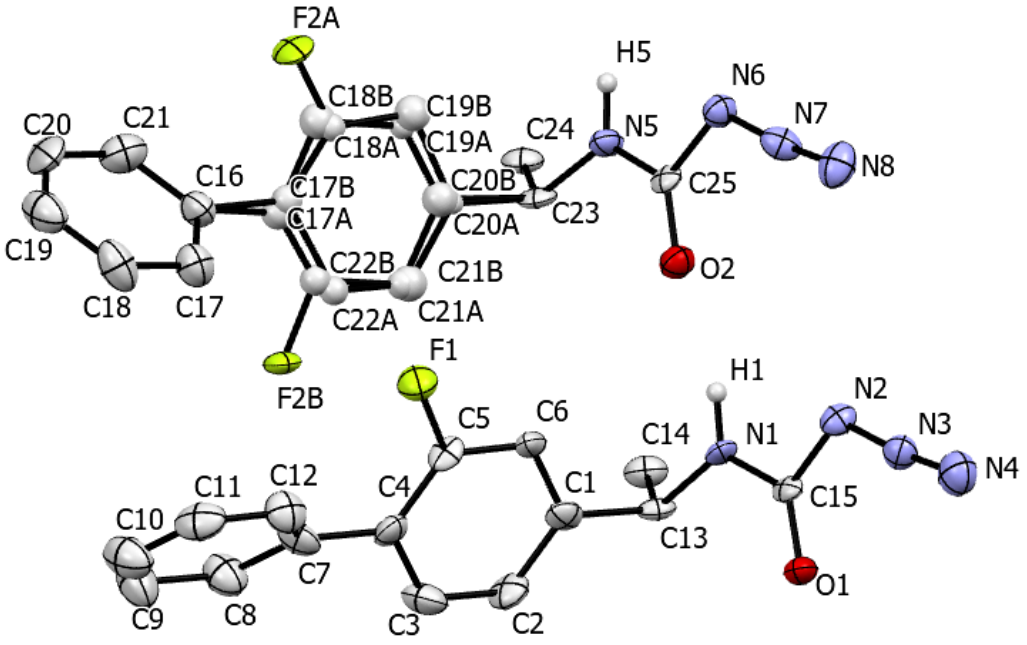

Fig. S20: ORTEP plot of **Flur-Az** (50% probability)

Table S5: Hydrogen bonding table for **Flur-Az**

D-H···A	d(D-H)/Å	d(H···A)/Å	d(D···A)/Å	∠D-H···A/°	Symmetry
N1-H1···O2	0.88	2.04	2.895(11)	164	x,-1+y,z

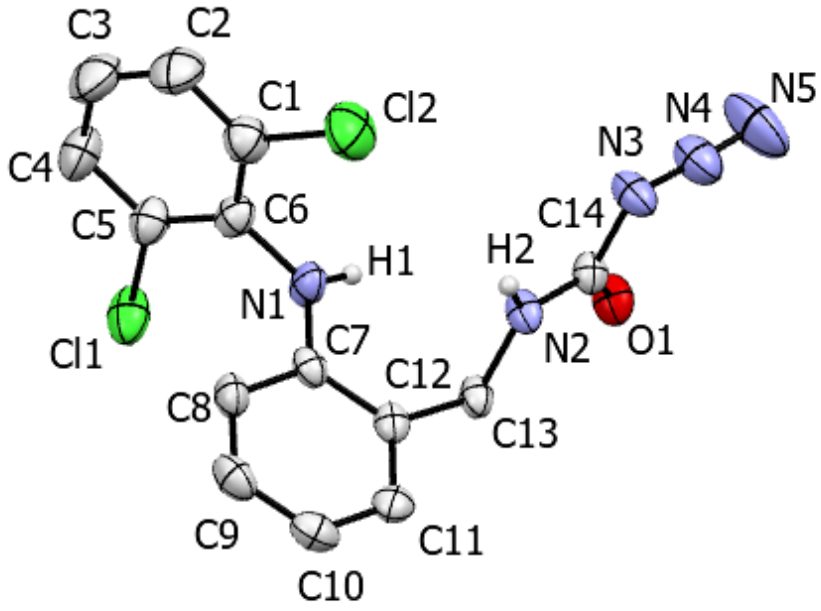

Fig. S21: ORTEP plot of **Diclo-Az** (50% probability)

Table S6: Hydrogen bonding table for **Diclo-Az**

D-H···A	d(D-H)/Å	d(H···A)/Å	d(D···A)/Å	∠D-H···A/°	Symmetry
N2-H2···O1	0.88	2.05	2.879(4)	156	x,1+y,z
N1-H1···Cl2	0.95	2.80	3.607(4)	144	x,1+y,z

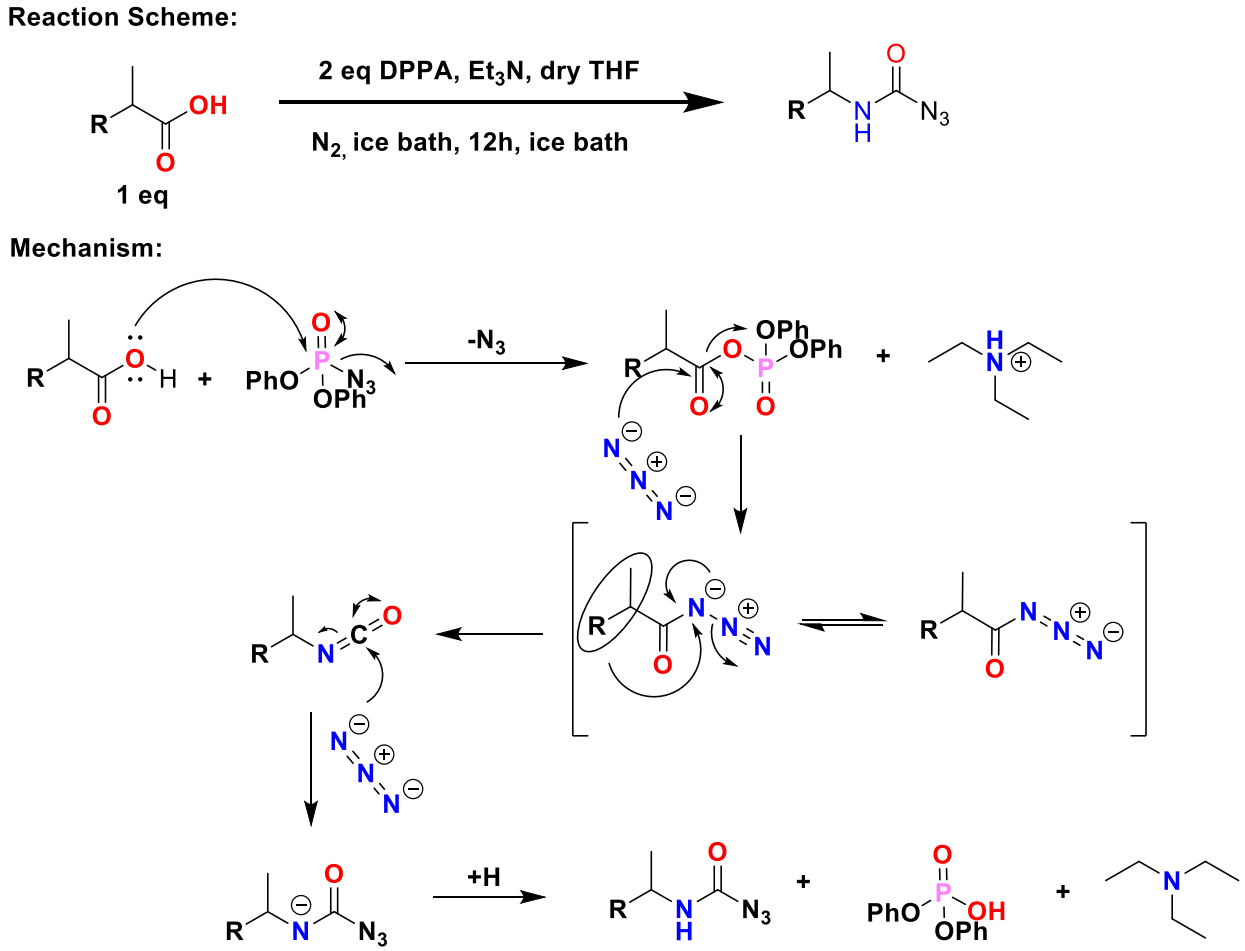

Fig. S22: Reaction Scheme and mechanism of carbamoyl azide.

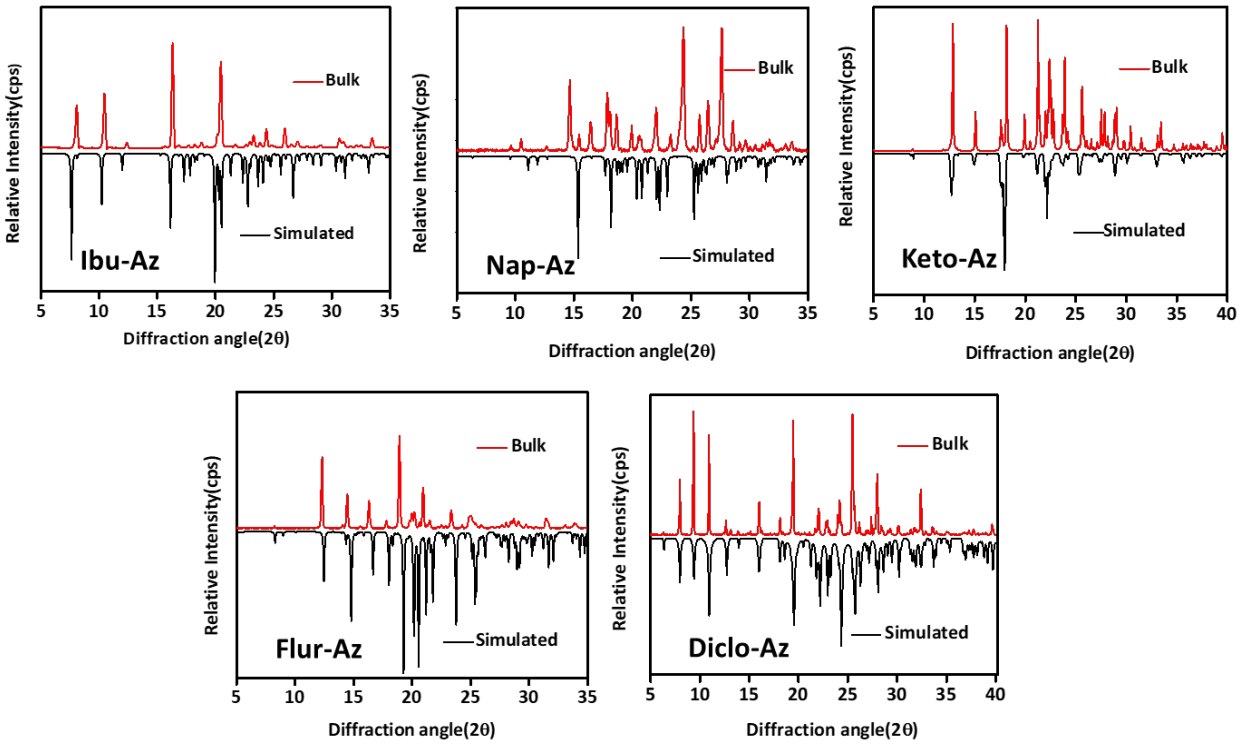

Fig. S23: PXRD plots of azides (bulk vs. simulated).

Table S7: Gelation table

Compound	Gelation Solvent (conc. 4 wt.% at RT)									
	DMSO:H_2O(1:1)	**WATER**	**DCM**	**THF**	**CH_3CN**	**DMSO**	**DMF**	**1,4-Dioxan**	**Methyl salicylate**	**Nitro-benzene**
Diclo-Az	**G**	INS	S	S	S	S	S	S	P	S
Nap-Az	**G**	INS	S	S	S	S	S	S	P	S
Flur-Az	GP	INS	S	S	S	S	S	S	S	S
Ibu-Az	P	INS	S	S	S	S	S	S	S	S
Keto-Az	S	INS	S	S	S	S	S	S	P	S
G=Gel, INS=Insoluble, S=Soluble, P=Precipitate, GP=Gelatinous Precipitate										

Table S8: M.G.C and tanδ (G”/G’**)** table

Gel	G” (Pa)	G’ (Pa)	tanδ (G”/G’)	Minimum Gelator Conc.(M.G.C)
Diclo-Az	444	8010	0.05	1.8 wt% (18mg/ml)
Nap-Az	774	9640	0.08	3.2wt% (32mg/ml)

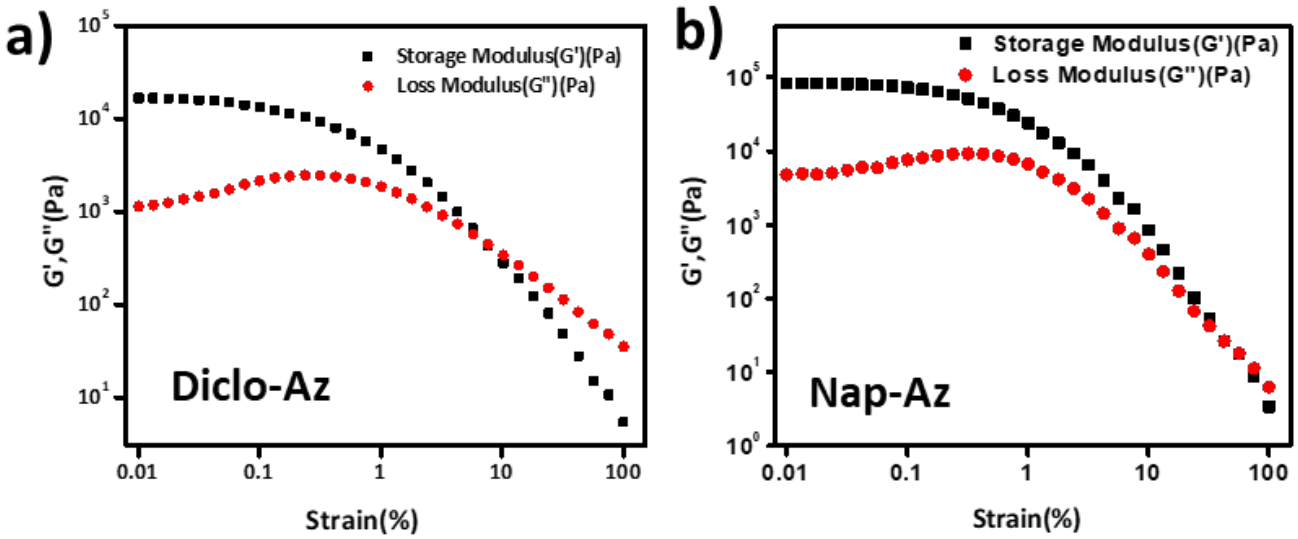

Fig. S24: Amplitude-sweep experiments of **4 wt.%** of **DMSO:H_2O (1:1)** gels: (a) **Diclo-Az** and (b) **Nap-Az**

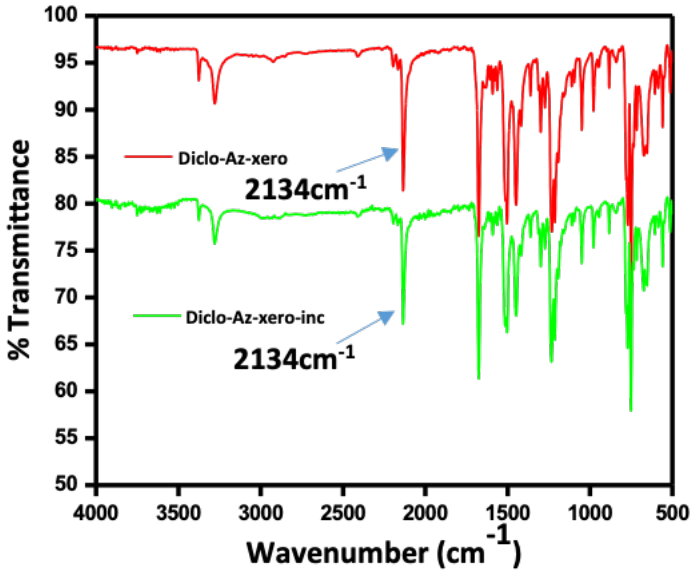

Fig. S25: FT-IR spectra of xerogel of **Diclo-Az** and xerogel of **Diclo-Az**-incubated at 37 °C for 24h.

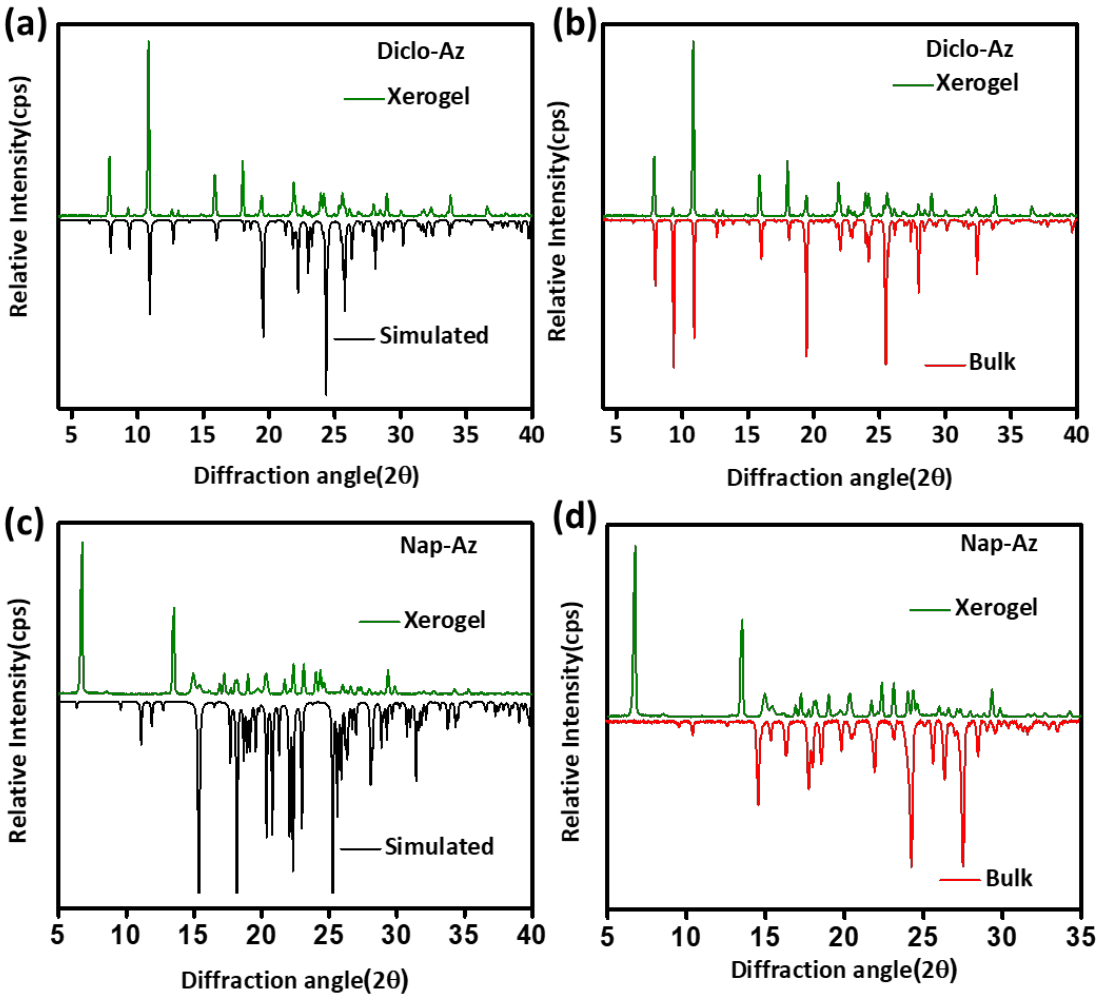

Fig. S26: PXRD Patterns (xerogel vs. bulk, xerogel vs. simulated) of (a, b) **Diclo-Az** and (c, d) **Nap-Az**

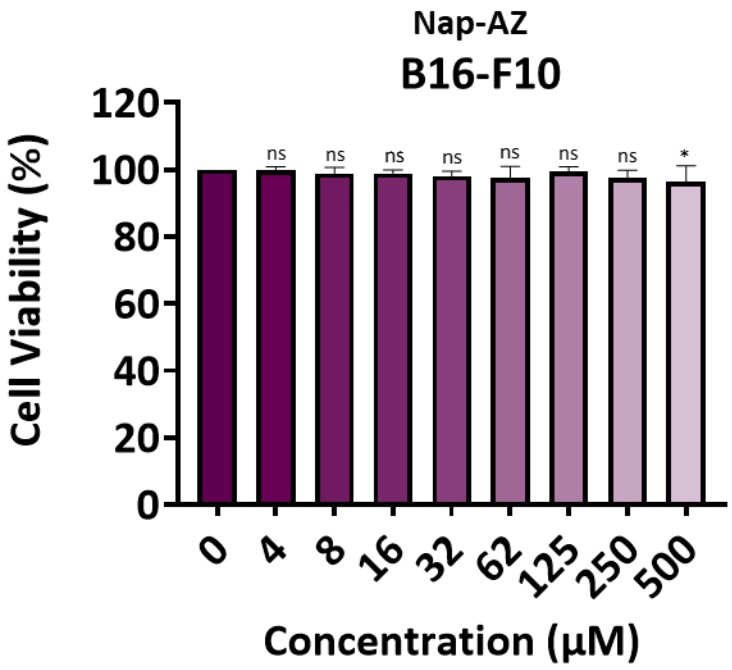

Fig. S27: MTT Assay on B16-F10 for **Nap-Az**. Data are represented considering mean ± SD of the replicates where *$P < 0.05$, **$P < 0.01$ and ***$P < 0.001$ and ns represents nonsignificant.

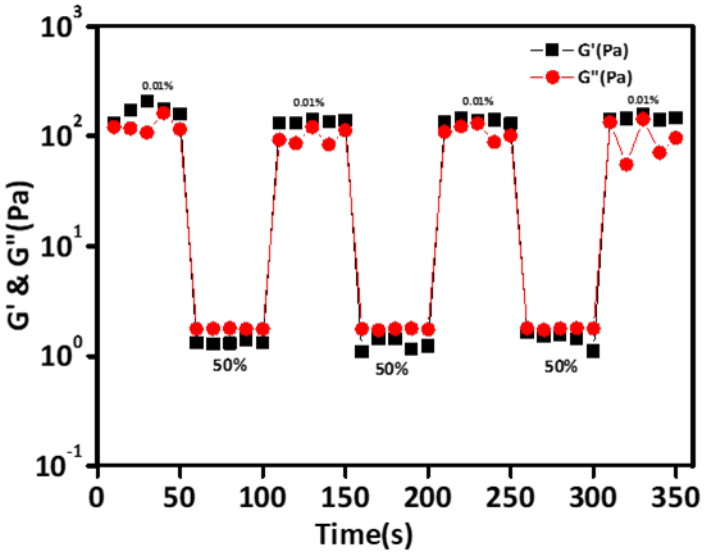

Fig. S28: Rheo-reversibility of **Nap-Az** (4 wt%, DMSO/water, 1:1, v/v)